

Development of a Damped Cavity with SiC Beam-Duct

T. Koseki, M. Izawa^{a)} and Y. Kamiya

Synchrotron Radiation Laboratory, The Institute for Solid State Physics (ISSP),
The University of Tokyo, Tanashi, Tokyo 188, Japan

a) Photon Factory, National Laboratory for High Energy Physics, Tsukuba, Ibaraki 305, Japan

abstract

The recent status of the R&D on a damped structure cavity being developed at ISSP and Photon Factory is presented. For the cavity, the higher-order modes (HOM's) damping is obtained with the large beam duct, a part of which is made of sintered SiC. A prototype cavity has been built and tested at low power levels. It was confirmed that the HOM's, which can propagate out of the cavity through the beam duct, were strongly damped by the SiC duct. Recently, fabrication of a high power model has been completed. High power conditioning of the model is now prepared.

I. INTRODUCTION

The damped cavity aims at being installed in two low emittance electron/position storage rings. One is a third-generation VUV and SX synchrotron radiation source being designed at ISSP [1] in collaboration with the Photon Factory (PF). The other is a high brilliance configuration of the PF storage ring [2]. The basic parameters of these storage rings are listed in Table 1.

Table 1: The basic parameters of the VUV and SX storage ring and PF high-brilliance configuration.

| | VUV-SX | PF |
|-----------------------------|---------|---------|
| Beam energy [GeV] | 2.0 GeV | 2.5 GeV |
| Lattice type | DBA | FODO |
| Circumference [m] | 374 | 187 |
| Revolution frequency [MHz] | 0.801 | 1.603 |
| Natural emittance [nm-rad] | 4.9 | 27 |
| RF frequency [MHz] | 500.1 | 500.1 |
| Harmonic number | 624 | 312 |
| Peak effective voltage [MV] | 1.5 | 1.5 |
| Energy loss / turn [keV] | 213.8 | 398.8 |
| Beam current [mA] | 400 | 500 |
| Bunch length [mm] | ~4 | ~10 |
| Number of the cavity | 3 | 4 |

The schematic of a quadrant of the cavity is shown in Fig. 1. The cavity has large beam duct, a part of which is made of sintered SiC. The HOM's propagating out from the cavity through the beam duct are then absorbed by the SiC parts[3,4].

The SiC material we adopted was CERASIC-B (pressureless sintered SiC made by Toshiba Ceramics Co. Ltd.), which has properties such as high thermal conductivity, a small outgassing rate, adequate mechanical strength and

suitable resistivity of 10 - 100 Ω -cm in the frequency range of a few GHz.

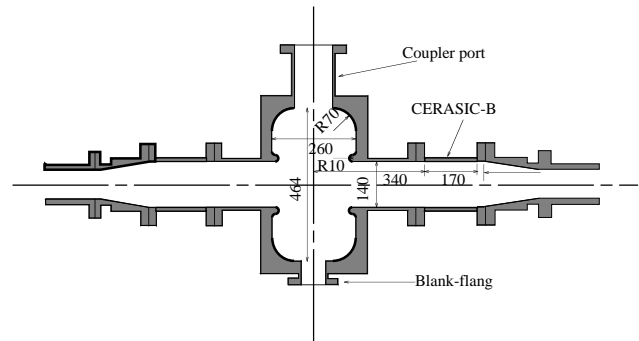


Figure 1: The cross sectional view of the damped cavity.

II. LOW POWER MEASUREMENT OF THE PROTOTYPE

We have fabricated the prototype model of the cavity and carried out its low power test. The model cavity itself was made of aluminum. Two types of beam ducts with the same length were prepared for the test. One was all made of aluminum and the other was partly made of CERASIC-B. The measured resistivity of the CERASIC-B duct was approximately 80 Ω -cm in the frequency region of 1.5 to 3.0 GHz.

The cavity has four ports, which are for an input coupler, a tuning plunger and two blank-flanges, respectively. We fabricated a cold model of newly designed input coupler with low VSWR at the operating frequency of 500.1 MHz [5]. The tuning plunger was the same type as used in the PF cavity. The blank-flange, also called fixed tuner, is a flange with cylindrical block to pad the port of the cavity. We measured the effects of block length on the resonance frequencies and Q-values of HOM's.

The measurement of RF characteristics was made with a network analyzer (HP8510C). For mode identification of HOM's, the field distributions in the cavity with aluminum beam duct were measured by the method of perturbation technique [3]. All modes predicted by the computer code URMEL were well identified.

A . HOM's above cutoff frequency of the beam-duct

The HOM's with frequencies higher than the cutoff of the 140 mm ϕ beam duct (1.64 GHz for TM₀₁ mode and 1.26 GHz for TE₁₁ mode) can propagate out from the cavity. It is therefore expected that they can be absorbed by CERASIC-B ducts. We then measured the transmission response (S₂₁) between two small rod antennas put at both endplates of the beam duct. Figure 2 and 3 show the measured spectrum from 1.5 GHz to 2.0 GHz. Figure 2 is the case of the aluminum beam duct and Fig. 3 the case of CERASIC-B beam duct. Similarly, Figures 4 and 5 show the spectrum from 2.0 GHz to 2.5 GHz. Figure 4 is the case of the aluminum beam duct and Figure 5 the case of CERASIC-B beam duct. The identified modes with URMEL notation are also indicated in Figs. 2 and 4. As shown in the figures, all resonances for the CERASIC-B beam duct were strongly damped and no longer visible.

B . Trapped modes

Since the HOM's with frequencies lower than the cutoff of the 140 mm ϕ beam duct are trapped in the cavity

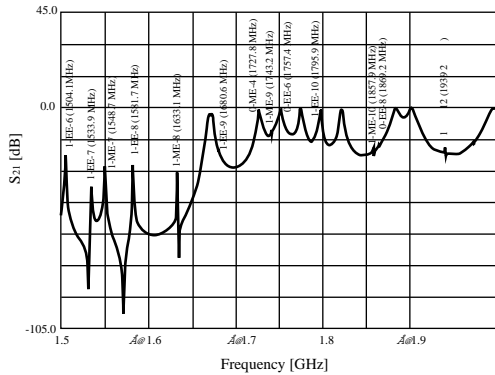


Figure 2: HOM's from 1.5 to 2.0 GHz for the Al beam duct.

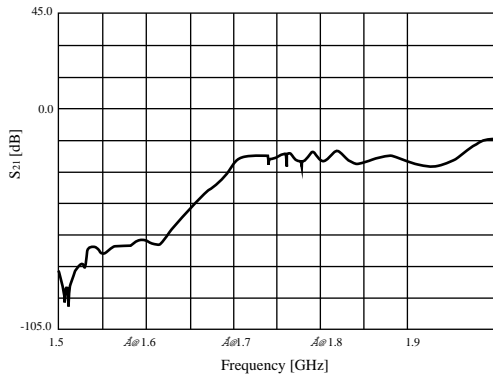


Figure 3: HOM's from 1.5 to 2.0 GHz for the SiC beam duct.

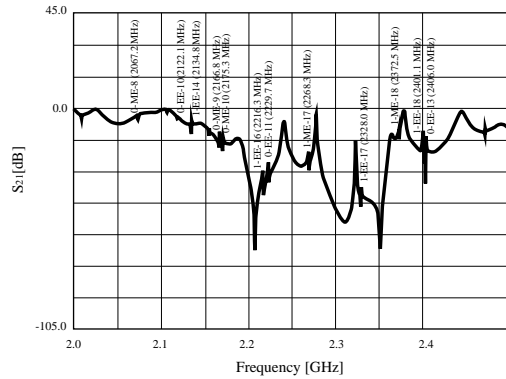


Figure 4: HOM's from 2.0 to 2.5 GHz for the Al beam duct.

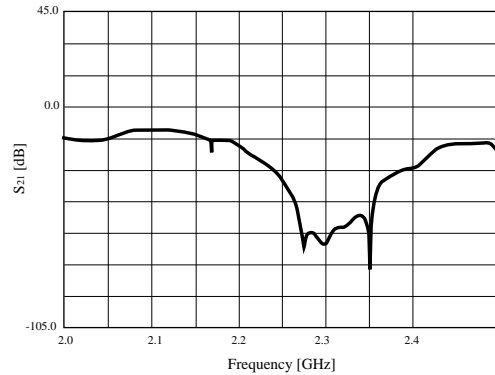


Figure 5: HOM's from 2.0 to 2.5 GHz for the SiC beam duct.

and they can not be absorbed in the CERASIC-B duct. The properties of these trapped modes are summarized in Tables 2 and 3. In order to avoid the instability due to these modes, two kind of methods may be applicable. One is the detuning of resonant frequencies of the HOM's by properly choosing the lengths of the blank-flanges [6], and the other is a bunch feedback method [7].

Figure 6 shows examples of the frequency dependence of HOM's on the length of blank-flange. The lengths in the figures are measured inward from the surface of the cavity. These data were taken under the following conditions; the frequency of accelerating mode was fixed at 500.1 MHz by adjusting the tuning plunger, and the length of one blank-flange was changed while that of the other was fixed. Figure 6(a) is for TM_{110h} modes and (b) for TM₀₁₁ mode. For TM_{110h} mode, the frequency detuning can be easily done since the frequency shift is sufficiently large. However, it would be difficult for TM₀₁₁ mode, because of its small frequency shift. Thus the feedback method should be applied for this kind of mode. The measured frequency shifts with the length of blank-flange for all trapped modes are also shown in Table 2 and 3.

Table 2: The properties of longitudinal trapped modes. Q_c indicates the Q-values for Cu estimated from the measured ones for Al. Δf is a frequency shift per 1mm change in the length of one blank-flange for the accelerating mode being fixed at 500.1 MHz.

| Mode type | URMEL notation | f [MHz] (meas.) | Q (calc.) | Q_c (meas.) | (Rs/Q) [Ω] (calc.) | Δf [kHz/mm] |
|-----------|----------------|-----------------|-----------|---------------|-----------------------------|---------------------|
| TM010 | 0-EE-1 | 500.1 | 43894 | 36000 | 175 | |
| TM011 | 0-ME-1 | 793.0 | 36554 | 28000 | 52.2 | 20 |
| | 0-EE-3 | 1310.0 | 56807 | 7000 | 9.28 | 10 |
| TM021 | 0-ME-2 | 1371.0 | 43051 | 11000 | 8.90 | 85 |

Table 3: The properties of transverse trapped modes.

| Mode type | URMEL notation | f [MHz] (meas.) | Q (calc.) | Q (meas.) | (Rt/Q) [Ω/m] (calc.) | Δf [kHz/mm] |
|-----------|----------------|-----------------|-----------|-----------|-------------------------------|---------------------|
| TE111 | 1-ME-1 | 704.6 | 45739 | 30000 | 7.40 | 150 |
| TM110V | 1-EE-1 | 789.7 | 49972 | 7000 | 248 | -100 |
| TM110H | 1-EE-1 | 792.6 | 49972 | 39000 | 248 | 100 |
| TM111H | 1-ME-2 | 988.8 | 27214 | 25000 | 449 | -90 |
| TM111V | 1-ME-2 | 989.8 | 27214 | 17000 | 449 | 120 |
| | | 991.3 | | 32000 | | 50 |

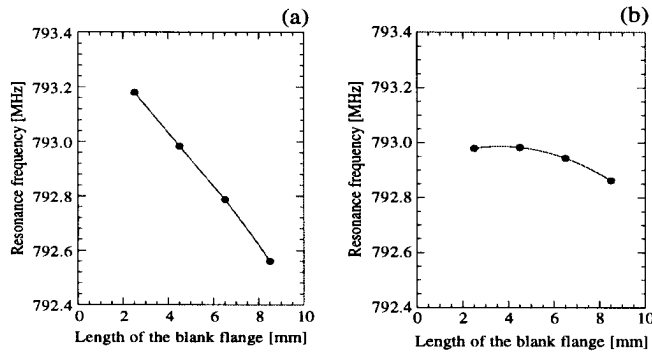


Figure 6: The frequency dependence of HOM on the length of blank-flange. (a) TM110h mode, (b) TM011 mode.

III. HIGH POWER MODEL

Recently, fabrication of a high power model has been completed. Figure 7 shows the model with a newly designed input coupler described in Ref.[5]. The model was manufactured at Keihin Product Operations of Toshiba Corporation. The main part of the high power model is made of OFHC copper. The unloaded Q value of the accelerating mode was measured to be 39000 at 500.1 MHz. The coupling coefficient β was 2.35, while the value expected from the low power measurement was 2.27 [5].

We have also fabricated the CERASIC-B duct for high power test. The duct is composed of Al duct with ICF253 flanges and CERASIC-B duct which is inserted in the Al duct by the method of shrink fit. The high power test of the CERASIC-B duct has been successfully carried out as described in Ref. [8].

The high power test of the cavity is being prepared. We will soon start its high power conditioning.

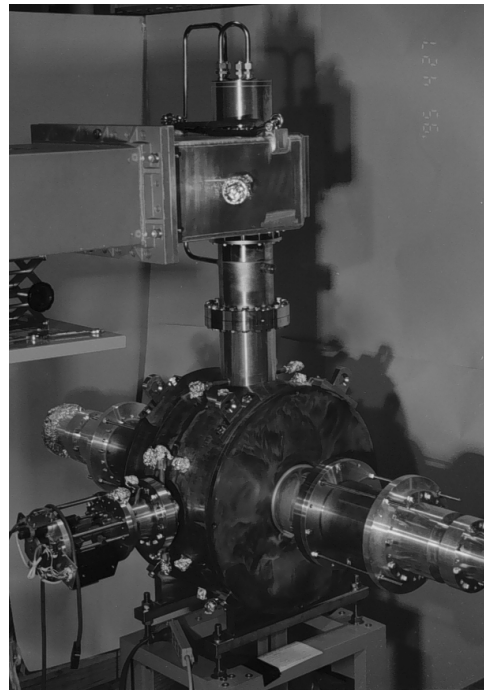


Figure 7: The high power model.

IV. REFERENCES

- [1] Y.Kamiya et al., Proc. 4th EPAC, London, 1994, p. 639.
- [2] M. Katoh et al., Rev. Sci. Instrum., 66 (1995) 1892.
- [3] T. Koseki et al., Proc. 4th EPAC, London, 1994, p. 2152.
- [4] T. Koseki et al., Rev. Sci. Instrum., 66(1995) 1926.
- [5] T. Nagatsuka, T. Koseki, Y. Kamiya, M. Izawa and Y. Terada, "A Design of Input Coupler for RF cavity" in these proceedings.
- [6] H. Kobayakawa et al., Rev. Sci. Instrum., 60(1989)1732.
- [7] E. Kikutani et al., Proc. 4th EPAC, London, 1994, p. 1613.
- [8] M. Izawa et al., Rev. Sci. Instrum., 66(1995) 1910.